Cancer Chemother Pharmacol (1996) 38: 117–122

ORIGINAL ARTICLE

Erika Cretton-Scott · Laurent Placidi
Harold McClure · Daniel · C. Anderson
Jean-Pierre Sommadossi

Pharmacokinetics and metabolism of *O*-(chloroacetyl-carbamoyl) fumagillol (TNP-470, AGM-1470) in rhesus monkeys

Received: 17 May 1995/Accepted: 9 October 1995

Abstract The metabolic disposition and pharmacokinetics of TNP-470 were investigated in rhesus monkeys following intravenous administration of 5 mg/kg of [^{3}H]-TNP-470. Rapid and extensive metabolism of parent drug to six metabolites occurred as demonstrated by the absence of unchanged drug in plasma and urine at time points as early as 6 min after administration. Substantial, yet variable, plasma levels of M-IV were detected in all three monkeys with a mean C_{max} value of 3.54 μM. Five other metabolites, labeled M-I, M-II, M-III, M-V and M-VI, were also detected in biological fluids of monkeys. M-II, M-V and M-VI exhibited similar kinetic profiles with apparent plasma elimination half-life values of 0.91 $\pm$ 0.37, 2.42 $\pm$ 0.13 and 1.19 $\pm$ 0.29 h respectively. In contrast, M-I, M-III and M-IV exhibited much shorter apparent plasma half-life values of 30 min or less. Urinary recovery within 36 h represented only 19.90 $\pm$ 6.09% of the total administered dose. No radioactivity was detected beyond 36 h and during a 15-day sample collection period, suggesting that nonrenal (biliary) elimination of TNP-470 metabolites is a predominant excretion route in nonhuman primates. This study provides the first detailed in vivo analysis of TNP-470 metabolism and disposition using an animal model highly predictive of humans, consistent with the detection of the same TNP-470 metabolites in human tissues. A detailed understanding of TNP-470 metabolism and disposition is critical to fully elucidate the pharmacodynamic properties of this new anticancer drug as clinical investigations proceed.

Key Words TNP-470 · Angiogenesis · Pharmacokinetics · Monkeys · Metabolism

E. Cretton-Scott · L. Placidi · J.-P. Sommadossi
Department of Pharmacology, Center for AIDS Research, Comprehensive Cancer Center, Division of Clinical Pharmacology, University of Alabama at Birmingham, Birmingham, Alabama 35294, USA

H. McClure · D.C. Anderson
Yerkes Regional Primate Research Center, Emory University, Atlanta, Georgia 30322, USA

J.-P. Sommadossi(✉)
Department of Pharmacology and Toxicology, University of Alabama at Birmingham, 1670 University Boulevard, Volker Hall G019, Birmingham, Alabama 35294, USA

Introduction

The development and dysregulated proliferation of blood vessels (endothelial cells, pericytes, mast cells) known as angiogenesis, is critical for growth and regrowth of common solid tumors. The discovery of antiangiogenic modulators presents a promising area in cancer chemotherapy, possibly providing a novel selective therapy for impairment of tumor growth. A new class of compounds known as angioinhibins has emerged from the discovery of an antibiotic, fumagillin, which exhibits potent antiangiogenic activity [10]. Unfortunately, fumagillin treatment is limited by important toxic side effects with prolonged administration [7, 11]. TNP-470 is a semisynthetic analogue of fumagillin that is 50 times more potent than its parent compound in inhibiting capillary growth with significantly less toxicity both in vitro and in vivo than the parent compound [4, 13, 19].

The recent demonstration by Saville et al. [18] that TNP-470 inhibits the growth of a spindle cell line derived from a Kaposi's sarcoma patient at a concentration that does not affect peripheral blood mononuclear cell proliferation has also led to the evaluation of TNP-470 for the treatment of Kaposi's sarcoma in AIDS patients.

In vitro studies by our group using primary cultured hepatocytes and microsomal fractions of various human tissues have demonstrated a rapid and extensive formation of at least six metabolites, two of which have

been identified and labeled as M-II and M-IV [16]. We have also determined that M-IV formation is associated with an esterase-like enzymatic cleavage of TNP-470 and that this metabolite is subsequently metabolized to M-II by microsomal epoxide hydrolase. These in vitro results emphasize further the need to elucidate the in vivo metabolism and disposition of TNP-470.

The purpose of the present study was to examine the pharmacokinetics and metabolism of TNP-470 in a nonhuman primate model. Although direct extrapolation of animal studies to the clinical situation should be made with caution, it should be noted that this model has been highly predictive of the pharmacokinetics of various compounds in humans including anticancer [1–3] and antiviral agents [5, 6].

Materials and methods

Drugs

Unlabeled TNP-470 and [^{3}H]-TNP-470 (3*R*, 4*S*, 5*S*, 6*R*)-5-methoxy-4-[(2*R*, 3*R*)-2-methyl-3-(3-methyl-2-butenyl)oxiranyl]-1-[6-^{3}H]oxaspiro-[2.5]-oct-6-yl-(chloroacetyl) carbamate (6 Ci/mmol) were supplied by Takeda Chemical Industries (Osaka, Japan), and were $>$ 96% pure as ascertained by the HPLC method described below. Unlabeled metabolite M-II (M-II, T-71712) and metabolite M-IV (M-IV, AGM-1883) authentic standards were also provided by the same company.

Animal experimental design

Rhesus monkeys (*Macaca mulatta*) were used for the metabolic and pharmacokinetic studies. The animals were maintained at the Yerkes Regional Primate Research Center of Emory University in accordance with guidelines established by the Animal Welfare Act and the National Institutes of Health Guide for the Care and Use of Laboratory Animals. The Yerkes Center is fully accredited by the American Association for Accommodation of Laboratory Animal Care. Prior to the start of the study, serum chemistry and hematology tests were performed to verify the health of the animals. Each monkey was identified by a tattooed number on the chest and was individually housed in a humidity- and temperature-controlled room with a 12:12 h light–dark cycle. The animals were fasted overnight prior to drug administration. On the dosing day, fresh drinking water was offered ad libitum and food provided 8 h after dosing. The animals were anesthetized with ketamine (10 mg/kg), with additional ketamine given as needed to maintain anesthesia.

Three young adult rhesus monkeys (RLa3, RMu2 and RBn3) weighing approximately 5.0 to 7.0 kg received one intravenous dose of 5 mg of TNP-470 per kg of body weight dissolved in sterile phosphate-buffered saline containing 10% ethanol to facilitate drug dissolution. A tracer amount of 250 μCi [^{3}H]-TNP-470 was admixed with the 'cold' dose to be administered. Blood samples (2 ml) were collected from the femoral vein into heparinized tubes at 0, 0.1, 0.17, 0.25, 0.5, 1, 1.5, 2, 3, 4, 6, 8 and 24 h after injection. Plasma was separated by centrifugation (300 *g*) and stored at -70°C with 2% sulfuric acid to ensure stability of TNP-470 and metabolites [8]. Urine was collected at similar times by cystocentesis for the first 8 h after which time the urine was pooled every 12 h until day 15 following drug administration. After measurement of volume, aliquots (10 ml) of urine were stored at -70°C with 2% sulfuric acid to ensure stability of TNP-470 and metabolites [8].

Sample analysis

Plasma samples (100 to 400 μl) were deproteinized with 2 volumes of acetonitrile by vortexing for 30 s, followed by centrifugation at 14 000 *g* for 5 min in an Eppendorf microcentrifuge. The supernatant was placed into a borosilicate glass tube and evaporated to dryness under a flux of nitrogen. The dried residue was redissolved in water and analyzed by HPLC. Urine samples (10 to 200 μl) were filtered through a 0.45 μm pore size Acro LC13 filter (Gelman Sciences, Ann Arbor, Mich.) prior to analysis.

The urinary and plasma profiles of unchanged drug and metabolites were determined by the same HPLC methodology. Analysis was performed using a Hewlett-Packard model 1050 liquid chromatograph equipped with a manual injector and a C_{18} Hypersil column (5 μm particle size, 4.6 × 250 mm; Jones chromatography, Littleton, Colo). Elution was performed at 1 ml/min with a 50 m*M* potassium phosphate monobasic buffer (pH 3) and a 40 min linear gradient of acetonitrile from 0 to 25% starting at the time of injection followed by an increase to 50% acetonitrile between 40 and 50 min. Absorbance was monitored at 210 nm. For plasma analysis, timed fractions of 1 ml were collected into miniscintillation vials over 60 min and after addition of 5 ml of Budget-Solve Scintillation fluor (Research Products International Corp., Mount Prospect, Ill.), radioactivity was measured in a TA 5000 liquid scintillation counter (Beckman Instruments, Palo Alto, Calif.). For urine analysis, radioactivity was determined using a 500 TR Radiomatic FLO-ONE radiochromatography analyzer (Packard Instrument Company, Meriden, CT.).

The total radioactivity applied to the column was recovered for all samples in 60 min (95 ± 5% recovery). The concentration of TNP-470 metabolites at each time point was determined by converting the recovered disintegrations per minute into picomoles of metabolite based on the specific activity of the dose administered. The detection limit of TNP-470 and metabolites was 0.05 μ*M* under these conditions. Retention times of TNP-470 and its metabolites M-IV and M-II were 58, 52 and 44 min, respectively. Four unidentified chromatographic peaks, labeled M-I, M-III, M-V and M-VI eluted at 48, 38, 30 and 27 min, respectively (Fig. 1). Intraday and interday coefficients of variation were less than 5% for all analyses. The standard curve for TNP-470 was linear, with $r^2 > 0.99$. However, the unavailability of radiolabeled metabolites did not permit the establishment of standard curves for these derivatives.

Pharmacokinetic analyses

The pharmacokinetic parameters of TNP-470 and metabolites were estimated by compartmental model-independent methods using a SIPHAR/Base program (SIMED, Creteil Cedex, France) [9]. Initial parameter estimates were determined using a curve-stripping algorithm with a two-compartment open model which assumed zero-order input and first-order elimination. Compartment model selection was based upon visual injection of the fit, evaluation of standard residual data comparison of the correlation coefficients and comparison of the coefficients of variation for the determined parameters. Final parameter estimates were determined using the terminal disposition slope (K) generated by a weighted least-squares algorithm with weighting set as the reciprocal of the calculated concentration squared [14]. The AUC was determined by the trapezoidal rule with extrapolation to time infinity. Elimination half-life ($t_{1/2}$) values of TNP-470 metabolites were calculated from $0.693/K$. The renal clearance, CL_R, of TNP-470 metabolites was determined by dividing the amount of each compound excreted in urine during a specified time period by the AUC corresponding to the same time

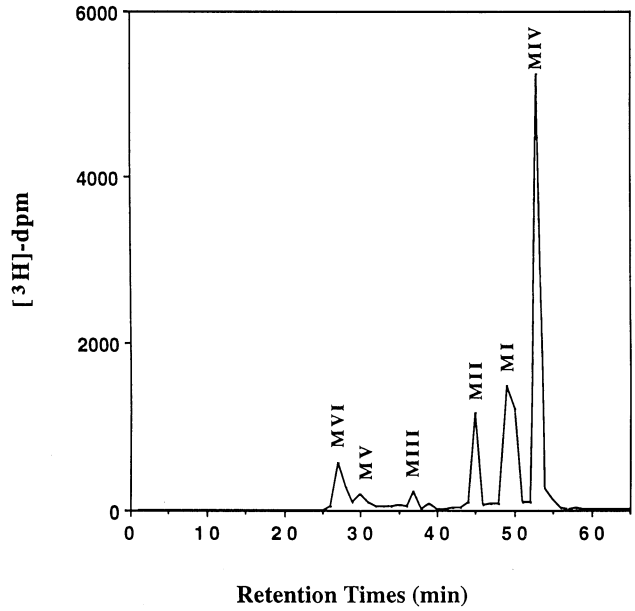

Fig. 1 HPLC profile of radioactivity in plasma 5 min after intravenous administration of 5 mg TNP-470 per kg. Resolution of TNP-470 metabolites was performed as described in Materials and methods

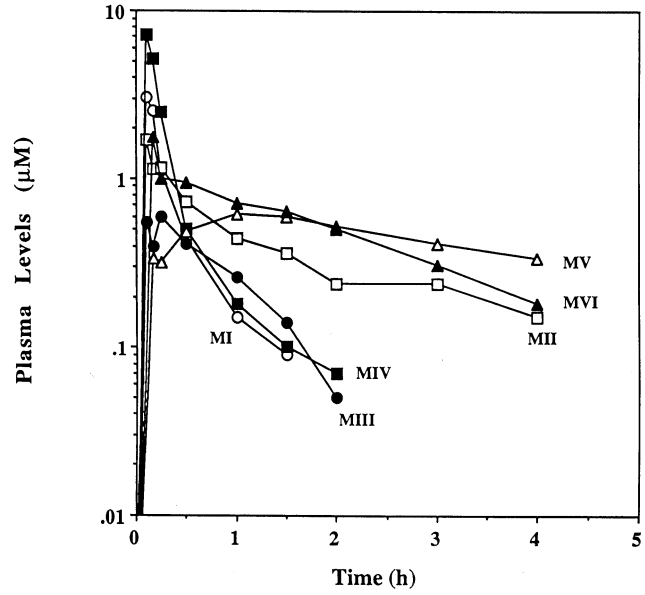

Fig. 2 Plasma concentration-time profiles of TNP-470 metabolites, M-I (○), M-II (□), M-III (●), M-IV (■), M-V (△) and M-VI (▲) in a representative monkey, RBn-2, after administration of 5 mg of TNP-470 per kg intravenously

period. The peak plasma concentration, C_{max}, values were observed experimental values.

Results

Kinetics of unchanged drug and metabolites in plasma

A representative plasma concentration-time profile of TNP-470 metabolites following intravenous administration of 5 mg drug per kg body weight to a monkey is illustrated in Fig. 2. Parent drug was undetectable in the plasma of all three animals whereas all six TNP-470 metabolite products were present in plasma as early as 6 min after drug administration, suggesting a rapid and extensive metabolism of TNP-470. The C_{max} values of M-IV were most variable while values of M-I, M-II, M-III, M-V and M-VI were quite consistent from animal to animal (Table 1). M-II, M-V and M-VI exhibited similar kinetic profiles with apparent plasma ($t_{1/2}$) mean (SD) values of 0.91 (0.37), 2.42 (0.13) and 1.19 (0.29) h, respectively. In contrast, M-I, M-III and M-IV exhibited much shorter plasma $t_{1/2}$ values of 30 min or less. Based on AUC values, M-V was the predominant plasma metabolite although only a two- to threefold difference in the AUC values was observed between this metabolite and the other TNP-470 metabolites (Table 1).

Urinary excretion of TNP-470 and metabolites

As observed for plasma (Figs. 1, 2), unchanged TNP-470 was not detected in urine at any time point. Metabolite M-IV was also not detected in urine of two monkeys (RLa3 and RMu2) but was detectable in the urine of RBn2 up to 10 min after drug administration, representing approximately 0.1% of the total radioactivity recovered in urine. It should be noted that plasma levels of M-IV in that monkey were substantially higher when compared to the other two animals (Table 1). In all three monkeys, excretion patterns for M-I, M-II, M-III, M-V and M-VI were similar, with most occurring between 0.5 and 2.0 h after TNP-470 administration. M-III, M-V and M-VI represented the bulk of the total radioactivity recovered, with M-V and M-VI being still detectable up to 24 h. M-II was also detectable up to 24 h in two monkeys (RLa3 and RBn2) whereas M-I was no longer detected after 4 h. Total urinary recovery ranged between 14.1% and 26.2% within 36 h (Table 2). Consistent with elevated CL_R values of TNP-470 metabolites, no radioactivity was detected beyond 36 h and during a 15-day sample collection period.

Discussion

Pharmacokinetic and metabolic studies were undertaken in a nonhuman primate model on the basis of a postulated metabolic pathway which included the conversion of TNP-470 to a metabolite M-IV through an esterase hydrolysis with further conversion of M-IV to M-II by microsomal epoxide hydrolase (Fig. 3) [16]. In the present study, the in vivo formation and disposition of these and other TNP-470 metabolites were examined through the administration of a radiolabeled

Table 1 Pharmacokinetic parameters after intravenous administration of 5 mg TNP-470 per kg in rhesus monkeys

Monkey	Compound	C_{max} (μM)	Apparent $t_{1/2}$ (h)	AUC (μM h)
RLa3	M-I	1.98	0.58	1.45
	M-II	0.78	1.03	1.18
	M-III	0.88	0.54	0.63
	M-IV	2.32	0.18	0.72
	M-V	0.30	2.44	1.32
	M-VI	0.77	1.23	1.62
RMu2	M-I	1.33	0.25	1.34
	M-II	1.09	0.49	1.07
	M-III	0.93	0.38	0.82
	M-IV	1.13	0.79	0.79
	M-V	0.78	2.29	1.92
	M-VI	0.65	0.88	1.44
RBn2	M-I	3.06	0.28	0.93
	M-II	1.70	1.20	1.91
	M-III	0.60	0.60	0.59
	M-IV	7.16	0.58	2.02
	M-V	0.62	2.54	3.10
	M-VI	1.00	1.45	2.44
Mean(SD)	M-I	2.12 (0.90)	0.37 (0.18)	1.24 (0.84)
	M-II	1.19 (0.47)	0.91 (0.37)	1.39 (0.46)
	M-III	0.80 (0.18)	0.51 (0.11)	0.68 (0.12)
	M-IV	3.54 (3.19)	0.52 (0.31)	1.18 (0.73)
	M-V	0.57 (0.24)	2.42 (0.13)	2.11 (0.91)
	M-VI	0.81 (0.18)	1.19 (0.29)	1.83 (0.53)

Table 2 Renal clearance and urinary excretion of TNP-470 metabolites after intravenous administration of 5 mg of TNP-470 per kg in rhesus monkeys (*NE* not evaluable)

Monkey	Compound	Amount (% of total dose)	Cl_R (ml/h/kg)
RLa3	M-I	2.53	207.93
	M-II	3.26	330.13
	M-III	6.04	1144.28
	M-IV	0.00	NE
	M-V	6.25	460.66
	M-VI	8.16	557.00
	Total	26.24	NE
RMu2	M-I	1.09	99.89
	M-II	1.46	168.22
	M-III	3.96	594.75
	M-IV	0.00	NE
	M-V	6.11	391.83
	M-VI	1.48	116.37
	Total	14.10	NE
RBn-2	M-I	1.35	180.56
	M-II	1.73	112.61
	M-III	4.14	873.04
	M-IV	0.15	8.60
	M-V	8.53	342.67
	M-VI	3.47	174.93
	Total	19.37	NE
Mean (SD)	M-I	1.66 (0.77)	162.79 (56.17)
	M-II	2.15 (0.97)	203.65 (113.01)
	M-III	4.71 (1.15)	870.69 (274.77)
	M-IV	NE	NE
	M-V	6.96 (1.36)	398.37 (59.30)
	M-VI	4.37 (3.43)	282.77 (239.29)

tracer amount of TNP-470 which permitted direct HPLC analysis with a limit of sensitivity of 0.05 μM, thus eliminating the need for extensive extraction steps that may have resulted in the loss of putative metabolites. Intravenous dosing was used to be consistent with the route of administration currently being studied in patients treated with TNP-470 [15, 17, 20].

Unchanged TNP-470 was rapidly and extensively metabolized in monkeys, as demonstrated by undetectable levels both in plasma and urine of monkeys receiving a 5 mg/kg dose of drug which is equivalent to a 57.6 mg/m^2 dose. These results are in agreement with those of preliminary human pharmacokinetic studies [8, 15] in which unchanged TNP-470 only achieved maximum plasma levels of 0.01 μM, a concentration below the sensitivity limit of the present methodology. Although it is conceivable that animal species, including rhesus monkeys, may metabolize TNP-470 at a faster rate, it should be noted that our in vitro studies using human hepatocytes also predicted accurately rapid and extensive metabolism [16].

Substantial plasma levels of M-IV were also detected in all three monkeys; however, a large variation was also noted in accordance with our in vitro studies using human liver microsomes [16] and metabolic studies of TNP-470 performed during a phase I dose escalation study [15]. In addition to M-IV, up to five metabolic derivatives, exhibiting the same HPLC retention times as those detected in human hepatocytes [16], were also detected in monkeys. The hypothesized metabolic pathway was confirmed in this in vivo study with the formation of the identified metabolite M-II (Fig. 1, 2). In the present study, M-II was not quantitatively as important as in human hepatocytes [16]. The in vitro minor metabolites, i. e. M-I, M-III, M-V and M-VI, were quantitatively as important as M-II in rhesus monkeys.

It is as yet unclear whether the quantitative difference between the results of the in vitro studies in human hepatocytes and the results of the studies in primates results from a species difference, or whether extrahepatic metabolism may also be a factor. In this context, microsomal epoxide hydrolase activity occurs predominantly in the liver rather than in other tissues [12], possibly explaining the quantitative importance of M-II in liver systems [16].

The present study provides the first detailed analysis of TNP-470 disposition and metabolism in a nonhuman primate model. The study demonstrated that TNP-470 is extensively metabolized in monkeys to six metabolites which have also been detected in a human cultured hepatocyte model [16]. Relevant to this study, analysis of plasma of patients receiving 10 to 30 mg/m^2 of TNP-470 has also demonstrated the presence of substantial levels of M-II and M-IV [15]. Although it is

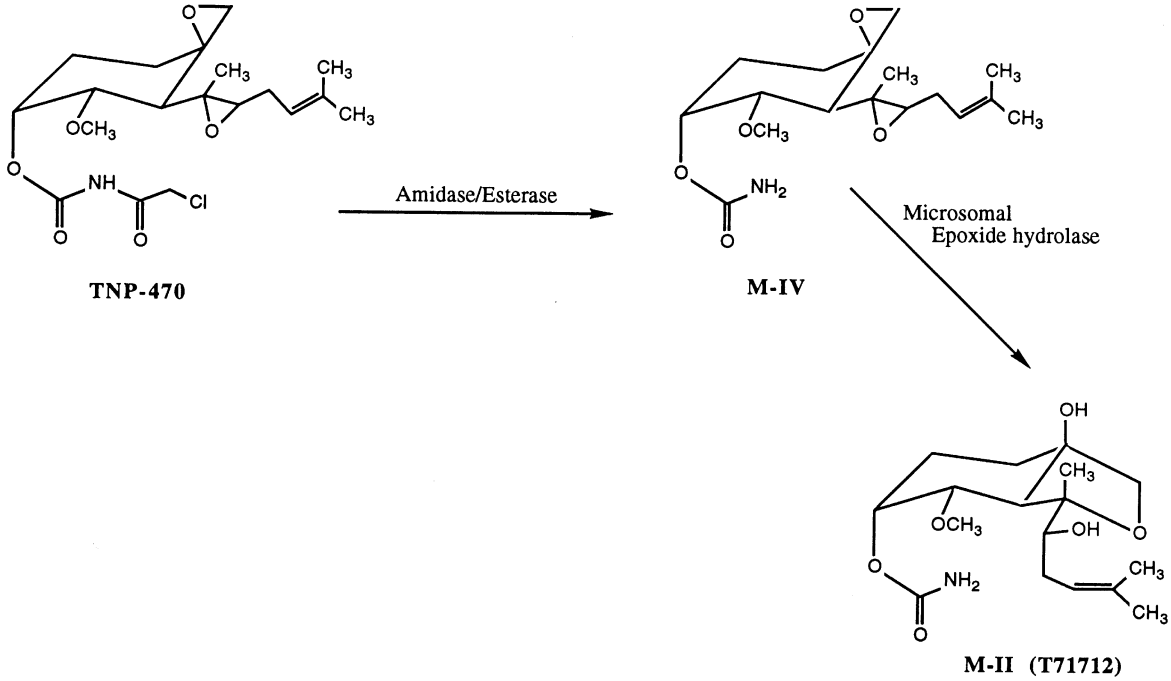

Fig. 3 Hypothesized metabolic pathways of TNP-470

as yet unknown whether the formation of M-I, M-III, M-V and M-VI occurs in humans, their detection after exposure of human tissues to TNP-470 and the investigated dose in monkeys being relevant to the doses studied in patients, may suggest that most of these TNP-470 derivatives should be formed in patients treated with TNP-470. Identification of these metabolites, i. e. M-I, M-III, M-V and M-VI, is in progress and will be reported at a later time.

Most of the administered dose in monkeys is probably excreted in feces although a complete mass-balance study will be necessary to precisely identify the distribution of the remaining radioactivity. A detailed understanding of TNP-470 metabolism and disposition will be important as clinical investigations with TNP-470 proceed. The rapid disappearance of TNP-470 combined with the substantial and variable formation of six other metabolites for which antiangiogenic activity is as yet unknown, suggests that such detailed pharmacokinetic and metabolism studies would also be needed in humans to fully understand the pharmacodynamic properties of this new anticancer drug with a novel mechanism of action.

Acknowledgements We would like to thank the staff of the Yerkes Regional Research Center for assisting with the monkey experiments. This work was supported in part by Public Health Service Grant, AI-32775, RR-00165 from the NIH, DHHS, and by an unrestricted grant from TAP Pharmaceuticals, Inc. J.-P. Sommadossi, Ph.D., is a recipient of a Faculty Research Award from the American Cancer Society.

References

1. Adamson PC, Balis FM, Arndt CA, Holcenberg JS, Narang PK, Murphy RF, Gillespie AJ, Poplack DG (1991) Intrathecal 6-mercaptopurine: preclinical pharmacology, Phase I/II trial, and pharmacokinetic study. Cancer Res 51:6079
2. Berg SL, Balis FM, McCully CL, Godwin KS, Poplack DG (1993) Pharmacokinetics of PEG-L-asparaginase and plasma and cerebrospinal fluid L-asparagine concentrations in the Rhesus monkey. Cancer Chemother Pharmacol 32:310
3. Blaney SM, Cole DE, Balis FM, Godwin K, Poplack DG (1993) Plasma and cerebrospinal fluid pharmacokinetic study of topotecan in nonhuman primates. Cancer Res 53:725
4. Brem H, Folkman J (1993) Analysis of experimental antiangiogenic therapy. J Pediator Surg 28:445
5. Cretton EM, Schinazi RF, McClure HM, Anderson DC, Sommadossi JP (1991) Pharmacokinetics of 3′-azido-3′-deoxythymidine and its catabolites and interactions with probenecid in rhesus monkeys. Antimicrob Agents Chemother 35:801
6. Cretton EM, Zhou Z, Kidd LB, McClure HM, Kaul S, Hitchcock MJM, Sommadossi JP (1993) In vitro and in vivo disposition and metabolism of 3′-deoxy-2′,3′-didehydrothymidine. Antimicrob Agents Chemother 37:1816
7. DiPaolo JA, Tarbell DS, Moore GE (1958–1959) Studies on the carcinolytic activity of fumagillin and some of its derivative. Antibiot Annu 541
8. Figg W, Yeh H, Thibault A, Pluda J, Itoh F, Yarchoan R, Cooper M (1994) Assay of the antiangiogenic compound, TNP-470, and one of its metabolites, AGM 1883, by reverse-phase, high performance liquid chromatography in plasma. J Chromatogr 652 (2):187
9. Gomeni R, Gomeni C (1978) Interactive graphic package for pharmacokinetic analysis. Comput Biomed Res 11:345
10. Ingber D, Fujita T, Kishimoto S, Sudo K, Kanamaru T, Folkman J (1990) Synthetic analogues of fumagillin that inhibit angiogenesis and suppress tumor growth. Nature 348:555

11. Killough JH, Magill GB, Smith RC (1952) The treatment of amoebiasis with fumagillin. Science 115 : 71
12. Krishna DR, Klotz U (1994) Extrahepatic metabolism of drugs in humans. Clin Pharmacokinet 26 : 144
13. Kusaka M, Sudo K, Fujita T, Marui S, Itoh F, Ingber D, Folkman J (1991) Potent anti-angiogenic action of AGM-1470: comparison to the fumagillin parent. Biochem Biophys Res Commun 174 : 1070
14. Marquardt DW (1963) An algorithm for least squares estimation of nonlinear parameters. J Soc Appl Math 11 : 431
15. Moore J, Sommadossi J-P and the AIDS Clinical Trial Group 215 Study Team (1995) Analysis of the angiogenic moderator *o*-(chloroacetyl-carbamoyl) fumagillol (TNP-470; AMG-1470) and metabolites in plasma by high performance liquid chromatography-mass spectrometry. Mass Spectrom (in press).
16. Placidi L, Cretton-Scott E, DeSousa G, Rhamani R, Placidi M, Sommadossi J-P (1995) Disposition and metabolism of the angiogenic moderator O-(chloroacetyl-carbamoyl) fumagillol (TNP-470; AGM-1470) in human hepatocytes and tissue microsomes. Cancer Res 55 : 3036
17. Pluda JM, Wyvill K, Figg WD, Whitcup SM, Lietzau J, Saville MN, Cohen R, Feigal E, Parks D, Foli A, Bailey J, Broder S, Yarchoan R (1994) A phase I study of an angiogenesis inhibitor, TNP-470 (AGM-1470), administered to patients (PTS) with HIV-associated Kaposi's sarcoma (KS). American Society of Clinical Oncology, Thirtieth Annual Meeting, Dallas, Tx.
18. Saville MW, Foli A, Broder S, Yarchoan R (1993) in vitro activity of TNP470, a novel angiogenesis inhibitor, in Kaposi's sarcoma (KS) related spindle cell lines. J Cell Biochem Suppl 17E : 22
19. Yanase T, Tamaru M, Fujita K, Kodama S, Tanaka K (1993) Inhibitory effect of angiogenesis inhibitor TNP-470 on tumor growth and metastasis of human cell lines in vitro and in vivo. Cancer Res 53 : 2566
20. Zukiwski A, Gutterman J, Bui C, Sella A, Ellerhoust J, Tu S, Amato R, Figg W, Kilbourn R, Logothetis C (1994) Phase I trial of the angiogenesis inhibitor TNP-470 (AGM-1470) in patients (PTS) with androgen independent prostate cancer (Al Pca). American Society of Clinical Oncology, Thirtieth Annual Meeting, Dallas, Tx.